Unstable modes of the Q1-P0 element

Griffiths, David and Silvester, David

2011

MIMS EPrint: **2011.44**

Manchester Institute for Mathematical Sciences
School of Mathematics

The University of Manchester

Reports available from: http://eprints.maths.manchester.ac.uk/
And by contacting: The MIMS Secretary
School of Mathematics
The University of Manchester
Manchester, M13 9PL, UK

ISSN 1749-9097

UNSTABLE MODES OF THE Q_1–P_0 ELEMENT

DAVID F. GRIFFITHS* AND DAVID J. SILVESTER †

Abstract. In this paper the unstable eigenmodes of Q_1–P_0 velocity/pressure finite element approximation for incompressible flow problems are characterised. It is shown that the inf-sup stability constant is $O(h)$ in two dimensions and $O(h^2)$ in three dimensions. The basic tool in the analysis is the method of modified equations which is applied to finite difference representations of the underlying finite element equations. The asymptotic estimates are confirmed and supplemented by numerical experiments.

1. Introduction. It is universally recognised that discretisation schemes for Stokes and Navier-Stokes equations are subject to an inf-sup or *div*-stability condition, see [2]. The stability requirement is manifested in practical computations by the predominance of staggered grid finite volume discretisations, and the existence of unnatural velocity–pressure finite element combinations. These typically involve velocity bubble functions, or else have a macro-element definition of the velocity field.

The "natural" (primitive variable) discretisations; non-staggered finite difference methods, low order conforming finite element methods like Q_1–P_0 (trilinear/bilinear velocity with constant pressure), and unstructured triangular finite volume discretisations (cell centered pressures with cell vertex velocities) all tend to be unstable. The ramifications of this are considerable, in particular, the need to be an "expert user" seems to have limited the acceptance of numerical simulation as an alternative to experimental testing. In contrast, the use of numerical techniques in solid mechanics is universal. The Q_1–P_0 finite element method is particularly controversial. Despite being damned by theoreticians after the discovery of "weakly singular" modes [1], Q_1–P_0 is widely used in practice. In writing this paper, we hope to reconcile these extreme views. For the first time a clean analysis of the instability mechanism is presented. This builds on and clarifies previous discussions, [2] pp.240ff, [10], [1], [9], [6] and yet, paradoxically, leads to an explanation as to why Q_1–P_0 invariably works well in practice.

The aim is to keep the paper as short as possible. Our results are divided into three sections. In Section 2 we give a precise analytic description of the weakly singular modes in the two dimensional case. Our analysis is confirmed and augmented by some numerical experiments presented in Section 3. We extend our analysis to cover three dimensional elements in Section 4. We also consider the important issue of the instability of L_2–projection methods based on Q_1–P_0 approximation. Such methods are commonly used in the solution of transient flow problems [4]. The important issue of optimal "stabilisation" of Q_1–P_0 is not addressed herein, (although our results clearly have implications in this regard). For further discussion on this aspect, see [11] and [5].

2. Approximation and Analysis. In this section we introduce the finite element approximation of the Stokes equations in two dimensions, and we proceed to describe a means of estimating the relevant constant in the inf-sup condition.

We consider the Stokes equations in the form

$$\begin{aligned} -\nabla^2\mathbf{u} + \nabla p &= \mathbf{f} \qquad \text{in } \Omega \\ \nabla\cdot\mathbf{u} &= 0 \qquad \text{in } \Omega \\ \mathbf{u} &= \mathbf{g} \qquad \text{on } \Gamma \end{aligned} \tag{1}$$

where $\Omega = (0,1)^2$ denotes the unit square with boundary Γ. An alternative formulation is discussed at the end of this section. Assuming a grid of $n \times n$ square elements $\mathcal{K}$, so that $h = 1/n$, approximation

* Mathematics Division, University of Dundee, DD1 4HN, dfg@maths.dund.ac.uk
† School of Mathematics, University of Manchester, M13 9PL, d.silvester@manchester.ac.uk.

based on the Q_1–P_0 element uses function spaces

$$\begin{aligned}\mathcal{V}_h &= \left\{ \mathbf{u} \in [H^1(\Omega)]^2 \,\middle|\, \mathbf{u}_{|\mathcal{K}} \in Q_1(\mathcal{K}) \quad \forall \mathcal{K} \in \Omega \right\}, \\ \mathcal{P}_h &= \left\{ p \in L_2(\Omega) \,\middle|\, p_{|\mathcal{K}} \in P_0(\mathcal{K}) \quad \forall \mathcal{K} \in \Omega \right\},\end{aligned} \tag{2}$$

for velocity and pressure, respectively, where $Q_1(\mathcal{K})$ is the space of bilinear functions and $P_0(\mathcal{K})$ is the space of constant functions on $\mathcal{K}$. Denoting the velocity space satisfying homogeneous boundary conditions by $\mathcal{V}_{h,0} = \mathcal{V}_h \cap H_0^1(\Omega)$, the finite element formulation is: find $\mathbf{u}_h \in \mathcal{V}_h$ which interpolate the data $\mathbf{u}_h = \mathbf{g}$ at boundary nodes and $p_h \in \mathcal{P}_h$ such that

$$\begin{aligned}(\nabla \mathbf{u}_h, \nabla \mathbf{v}) + (\nabla p_h, \mathbf{v}) &= (\mathbf{f}, \mathbf{v}), \qquad \forall \mathbf{v} \in \mathcal{V}_{h,0} \\ -(q, \nabla \cdot \mathbf{u}_h) &= 0, \qquad \forall q \in \mathcal{P}_h.\end{aligned} \tag{3}$$

With standard interpolating bases for the spaces $\mathcal{V}_h$ and $\mathcal{P}_h$, this leads to the matrix system

$$\begin{pmatrix} A & 0 & B_x^t \\ 0 & A & B_y^t \\ B_x & B_y & 0 \end{pmatrix} \begin{pmatrix} \mathbf{U} \\ \mathbf{V} \\ \mathbf{P} \end{pmatrix} = \begin{pmatrix} \mathbf{F}_x \\ \mathbf{F}_y \\ \mathbf{G} \end{pmatrix}, \tag{4}$$

where $\mathbf{U}, \mathbf{V} \in I\!R^{n_u}$ contain the nodal values of the x and y components of the approximation to $\mathbf{u}_h$ at the internal vertices, and $\mathbf{P} \in I\!R^{n_p}$ contains the element centroid values of the pressure approximation. The matrix A is of order $n_u \times n_u$, while both B_x^t and B_y^t are of order $n_u \times n_p$, with $n_u = (n-1)^2$ and $n_p = n^2$.

The satisfaction of the inf-sup condition is dependent on the eigenvalues σ of

$$BK^{-1}B^t\mathbf{P} = \sigma M\mathbf{P} \tag{5}$$

(see [8]) where $M = h^2 I$ is the $n_p \times n_p$ mass matrix corresponding to the pressure space, $B = [B_x \; B_y]$ represents the discrete divergence operator and K is the vector Laplacian

$$K = \begin{pmatrix} A & 0 \\ 0 & A \end{pmatrix}.$$

Since the discrete velocity field is specified everywhere on the boundary, the discrete Stokes operator has a two-dimensional nullspace spanned by the hydrostatic and chequerboard pressure modes [10]. Consequently, (5) has only $n^2 - 2$ non–zero eigenvalues and we can order the eigenvalues so that

$$0 = \sigma_1 = \sigma_2 < \sigma_3 \leq \sigma_4 \leq \cdots \leq \sigma_{n^2}.$$

It may also be shown [8], that the nonzero eigenvalues of the "dual" problem

$$B^t M^{-1} B \begin{pmatrix} \mathbf{U} \\ \mathbf{V} \end{pmatrix} = \sigma K \begin{pmatrix} \mathbf{U} \\ \mathbf{V} \end{pmatrix} \tag{6}$$

coincide with those of (5). We shall find it more convenient to work with the related eigenproblem

$$\begin{pmatrix} A & 0 & B_x^t \\ 0 & A & B_y^t \\ B_x & B_y & 0 \end{pmatrix} \begin{pmatrix} \mathbf{U} \\ \mathbf{V} \\ \mathbf{P} \end{pmatrix} = \lambda \begin{pmatrix} A & 0 & 0 \\ 0 & A & 0 \\ 0 & 0 & M \end{pmatrix} \begin{pmatrix} \mathbf{U} \\ \mathbf{V} \\ \mathbf{P} \end{pmatrix} \tag{7}$$

which reduces to (5) on elimination of $\mathbf{U}$ and $\mathbf{V}$ and to (6) on elimination of $\mathbf{P}$. This system has an eigenvalue $\lambda = 1$ of multiplicity equal to the dimension of the nullspace of the discrete divergence operator, that is $(n-2)^2$, and the remaining $2(n^2-2)$ eigenvalues are generated by the quadratic equation $\lambda(\lambda - 1) = \sigma_j$ for $j = 3, \ldots, n^2$:

$$\lambda_j^- = \frac{1 - \sqrt{1 + 4\sigma_j}}{2} \leq 0 \qquad \text{and} \quad \lambda_j^+ = \frac{1 + \sqrt{1 + 4\sigma_j}}{2} \geq 1. \tag{8}$$

Applying the analysis of Brezzi and Fortin ([2], sec II.3.2) or Malkus[8] the inf-sup stability of the system (3) (or, equivalently, (4)) is determined by the square root of the smallest nonzero eigenvalue of (5) that is

$$\sqrt{\sigma_3} = \sqrt{\lambda_3^-(\lambda_3^- - 1)} \tag{9}$$

and we shall, accordingly, refer to λ_3^- as the critical eigenvalue of (7) and denote it by λ^*. Experimental evidence reported in [2] (Section VI.5.4) suggests that $\sigma_3 \to 0$ as $h \to 0$ indicating that Q_1–P_0 is not div-stable in general. To investigate this issue further we write the constituent equations of (7) in finite difference form and then appeal to the method of modified equations. This will allow us to establish the precise behaviour of σ_3 for small values of h.

The x and y components of velocity at the grid point $(\ell h, mh), \ell, m = 1, 2, \ldots, n-1$ are labelled $U_{\ell,m}, V_{\ell,m}$, respectively. The pressure is defined at element centroids $(\ell + 1/2)h, (m + 1/2)h), \ell, m = 0, 1, \ldots, n-1$ and is consequently labelled $P_{\ell+1/2,m+1/2}$. The system of equations (7) (each divided by h^2) may then be expressed as

$$\begin{aligned} -(1-\lambda)\nabla_h^2 U_{\ell,m} + h^{-1}\delta_x\mu_y P_{\ell,m} &= 0, \\ -(1-\lambda)\nabla_h^2 V_{\ell,m} + h^{-1}\mu_x\delta_y P_{\ell,m} &= 0, \\ -h^{-1}\delta_x\mu_y U_{\ell+1/2,m+1/2} - h^{-1}\mu_x\delta_y V_{\ell+1/2,m+1/2} &= \lambda P_{\ell+1/2,m+1/2}, \end{aligned} \tag{10}$$

where

$$\delta_x P_{\ell,m} = P_{\ell+1/2,m} - P_{\ell-1/2,m}, \qquad \mu_x P_{\ell,m} = \tfrac{1}{2}\left[P_{\ell+1/2,m} + P_{\ell-1/2,m}\right]$$

are the usual central difference and averaging operators, respectively, and ∇_h^2 denotes the discrete Laplacian generated by bilinear elements

$$\nabla_h^2 U_{\ell,m} = h^{-2}\left[\delta_x^2 + \delta_y^2 + \tfrac{1}{3}\delta_x^2\delta_y^2\right] U_{\ell,m}. \tag{11}$$

Associated with (10) we have the boundary conditions $U_{\ell,m} = V_{\ell,m} = 0$ at nodes lying on the boundary Γ. The system (10) is consistent to $\mathcal{O}(h^2)$ with the continuous eigenvalue problem

$$\begin{aligned} -\nabla^2\mathbf{u} + \nabla p &= -\lambda\nabla^2\mathbf{u} \qquad \text{in } \Omega, \\ -\nabla\cdot\mathbf{u} &= \lambda p \qquad \text{in } \Omega, \\ \mathbf{u} &= \mathbf{0} \qquad \text{on } \Gamma, \end{aligned} \tag{12}$$

which has one eigenvalue $\lambda = 0$ corresponding to the hydrostatic mode $\mathbf{u} = \mathbf{0}$, $p =$ constant, an eigenvalue $\lambda = 1$ of infinite multiplicity with corresponding eigenfunctions satisfying $\nabla\cdot\mathbf{u} = 0$, $p = 0$, and a pair of eigenvalues $\lambda = (1 \pm \sqrt{5})/2$ of infinite multiplicity corresponding to $\sigma = 1$ and having irrotational eigenvectors ($\nabla \times \mathbf{u} = 0$).

In order to study the behaviour of the critical eigenvalue λ^*, we assume that the corresponding eigenfunctions are highly oscillatory and have (smooth) envelopes $(\bar{U}, \bar{V}, \bar{P})$ defined by

$$\begin{aligned} U_{\ell,m} = h^2(-1)^{\ell+m}\bar{U}_{\ell,m}, \qquad V_{\ell,m} = h^2(-1)^{\ell+m}\bar{V}_{\ell,m}, \\ P_{\ell+1/2,m+1/2} = (-1)^{\ell+m+1}\bar{P}_{\ell+1/2,m+1/2}. \end{aligned} \tag{13}$$

It then follows that

$$\delta_x^2 U_{\ell,m} = h^2(-1)^{\ell+m+1}(4 + \delta_x^2)\bar{U}_{\ell,m} \tag{14}$$

so that

$$\nabla_h^2 U_{\ell,m} = \tfrac{1}{3}(-1)^{\ell+m+1}\left[8 - \delta_x^2 - \delta_y^2 - \delta_x^2\delta_y^2\right]\bar{U}_{\ell,m}. \tag{15}$$

Moreover,

$$\begin{aligned}
\delta_x\mu_y P_{\ell,m} &= (-1)^{\ell+m+1}\mu_x\delta_y\bar{P}_{\ell,m},\\
\mu_x\delta_y P_{\ell,m} &= (-1)^{\ell+m+1}\delta_x\mu_y\bar{P}_{\ell,m},\\
\delta_x\mu_y U_{\ell+1/2,m+1/2} &= h^2(-1)^{\ell+m}\mu_x\delta_y\bar{U}_{\ell+1/2,m+1/2},\\
\mu_x\delta_y V_{\ell+1/2,m+1/2} &= h^2(-1)^{\ell+m}\delta_x\mu_y\bar{V}_{\ell+1/2,m+1/2}.
\end{aligned}$$

When these relations are used to change dependent variables in (10) from (U,V,P) to $(\bar{U},\bar{V},\bar{P})$ we find that

$$\begin{aligned}
\tfrac{1}{3}(1-h^2\mu)\left[8-\delta_x^2-\delta_y^2-\delta_x^2\delta_y^2\right]\bar{U}_{\ell,m}-h^{-1}\delta_y\mu_x\bar{P}_{\ell,m}&=0,\\
\tfrac{1}{3}(1-h^2\mu)\left[8-\delta_x^2-\delta_y^2-\delta_x^2\delta_y^2\right]\bar{V}_{\ell,m}-h^{-1}\mu_y\delta_x\bar{P}_{\ell,m}&=0,\\
h^{-1}\delta_y\mu_x\bar{U}_{\ell+1/2,m+1/2}+h^{-1}\mu_y\delta_x\bar{V}_{\ell+1/2,m+1/2}&=\mu\bar{P}_{\ell+1/2,m+1/2},
\end{aligned}\tag{16}$$

where $\mu=\lambda/h^2$, together with homogeneous Dirichlet boundary conditions on $\bar{U}$ and $\bar{V}$.

Denoting the Q_1 basis function at node $(\ell h, mh)$ by $\phi_{\ell,m}$, and supposing that $\mathbf{u}_h=[u_h,v_h]\in\mathcal{V}_h$ has nodal values $[U_{\ell,m},V_{\ell,m}]$, then, since $(\nabla\phi_{\ell,m},\nabla u_h)=h^2\nabla_h^2U_{\ell,m}$ and $(\phi_{\ell,m},u_h)=h^2(1+\frac{1}{6}\delta_x^2)(1+\frac{1}{6}\delta_y^2)U_{\ell,m}$, it is easy to see that (16) is the Q_1–P_0 discretisation of the modified system

$$\begin{aligned}
\tfrac{1}{3}(1-h^2\mu)\left[8\bar{u}-\tfrac{7}{3}h^2\nabla^2\bar{u}-\tfrac{4}{9}h^2\bar{u}_{xxyy}\right]-\bar{p}_y&=0 \qquad \text{in } \Omega\\
\tfrac{1}{3}(1-h^2\mu)\left[8\bar{v}-\tfrac{7}{3}h^2\nabla^2\bar{v}-\tfrac{4}{9}h^2\bar{v}_{xxyy}\right]-\bar{p}_x&=0 \qquad \text{in } \Omega\\
\bar{u}_y+\bar{v}_x&=\mu\bar{p} \qquad \text{in } \Omega\\
\bar{u}=\bar{v}&=0 \qquad \text{on } \Gamma.
\end{aligned}\tag{17}$$

In the limit $h\to 0$ we obtain the reduced problem

$$\begin{aligned}
\tfrac{8}{3}\bar{u}-\bar{p}_y&=0 \qquad \text{in } \Omega,\\
\tfrac{8}{3}\bar{v}-\bar{p}_x&=0 \qquad \text{in } \Omega,\\
\bar{u}_y+\bar{v}_x&=\mu\bar{p} \qquad \text{in } \Omega,\\
\bar{u}=\bar{v}&=0 \qquad \text{on } \Gamma
\end{aligned}\tag{18}$$

which implies that

$$\nabla^2\phi-\tfrac{8}{3}\mu\phi=0 \qquad \text{in } \Omega \tag{19}$$

for each of the dependent variables $\phi=\bar{u},\bar{v},\bar{p}$. This, being a second order elliptic eigenvalue problem, requires only one boundary condition whereas the system (18) contains two. The equations (17) therefore represent a singularly perturbed system (see, for example, [7]) whose solutions will, in general, contain boundary layers. Bearing this in mind, we may identify the smallest nonzero eigenvalue of (17) as

$$\mu=-\tfrac{3}{8}\pi^2+\mathcal{O}(h)$$

associated with which there are two eigenfunctions, having outer expansions

$$\begin{pmatrix}\bar{u}_1\\ \bar{v}_1\\ \bar{p}_1\end{pmatrix}=\begin{pmatrix}\mu\sin\pi y\\ 0\\ \pi\cos\pi y\end{pmatrix},\qquad \begin{pmatrix}\bar{u}_2\\ \bar{v}_2\\ \bar{p}_2\end{pmatrix}=\begin{pmatrix}0\\ \mu\sin\pi x\\ \pi\cos\pi x\end{pmatrix}. \tag{20}$$

It is important to note that since $\bar{u}_1=0$ on Γ, it exhibits boundary layers of width $\mathcal{O}(h)$ along the vertical boundaries $x=0,1$. Similarly, $\bar{v}_2$ has boundary layers of width $\mathcal{O}(h)$ along the horizontal boundaries

$y = 0, 1$. We also note that, for this modified system, a "pressure gradient" in the y–direction induces a "flow" in the x–direction and vice–versa. We summarise in the form of a theorem.

THEOREM 1. *The critical eigenvalue of (7) is given by* $\lambda^* = -\frac{3}{8}\pi^2 h^2 + \mathcal{O}(h^3)$ *and the inf-sup constant for* Q_1–P_0 *elements is given by*

$$\sqrt{\sigma_3} = \sqrt{\tfrac{3}{8}}\pi h + \mathcal{O}(h^2).$$

The eigenspace corresponding to λ^* *has dimension two and is spanned by mutually orthogonal eigenvectors given, approximately, by*

$$\begin{pmatrix} U_{\ell,m} \\ V_{\ell,m} \\ P_{\ell+1/2,m+1/2} \end{pmatrix} = (-1)^{\ell+m+1} \begin{pmatrix} \frac{3}{8}\pi^2 h^2 \sin \pi m h \\ 0 \\ \pi \cos \pi(m+1/2)h \end{pmatrix} \tag{21}$$

and

$$\begin{pmatrix} U_{\ell,m} \\ V_{\ell,m} \\ P_{\ell+1/2,m+1/2} \end{pmatrix} = (-1)^{\ell+m+1} \begin{pmatrix} 0 \\ \frac{3}{8}\pi^2 h^2 \sin \pi \ell h \\ \pi \cos \pi(\ell+1/2)h \end{pmatrix} \tag{22}$$

at internal nodes of the domain and $U_{\ell,m} = V_{\ell,m} = 0$ *at boundary nodes.*

The amplitudes of the velocity and pressure contributions to these critical eigenvectors differ by a factor $\mathcal{O}(h^2)$, which explains why, in computations, the instabilities manifest themselves most strongly in the pressure field. This will be explored further in the next section in connection with the model lid driven cavity problem.

An alternative Stokes formulation to (1) is the stress divergence form (see [2] pp.13):

$$\begin{aligned} -\nabla^2 \mathbf{u} - \nabla(\nabla \cdot \mathbf{u}) + \nabla p &= \mathbf{f} \qquad \text{in } \Omega \\ \nabla \cdot \mathbf{u} &= 0 \qquad \text{in } \Omega \\ \mathbf{u} &= \mathbf{g} \qquad \text{on } \Gamma \end{aligned} \tag{23}$$

which after discretisation gives a matrix system which is slightly different to (4) above. If we discretise (23) using Q_1–P_0 and follow the procedure described by (13) for changing variables, then it easily shown that the resulting reduced problem is also of the form (18) except that the factor 8/3 is replaced by 4. In this case we have the result stated below.

THEOREM 2. *The inf-sup constant for* Q_1–P_0 *approximation of (23) is given by*

$$\sqrt{\sigma_3} = \tfrac{1}{2}\pi h + \mathcal{O}(h^2).$$

The corresponding eigenspace has dimension two and is spanned by mutually orthogonal eigenvectors given, approximately, by (21) and (22).

3. Numerical Experiments. In this section, we present some computational results indicating that the asymptotic analysis of Section 2 correctly predicts the behaviour of the critical eigenvalues of (7), for representative values of h. All computations presented here were performed using MATLAB 4.1 on a SUN Sparcstation–10.

We first consider the critical eigenvalue of Theorem 1. To this end, we solve the stability eigenproblem (5) analysed above, that is, using a Q_1–P_0 finite element subdivision of $n \times n$ square elements. The numerically computed eigenvalues σ_j are presented in Table 1. The smallest eigenvalues are clearly tending to zero like $O(h^2)$. The largest eigenvalue is converging to a asymptotic limit of unity. To confirm the eigenvalue estimate given in Theorem 1, the quantity $-(\frac{8}{3})\lambda^*/(\pi h)^2$ is plotted as a function

of h in Figure 1. As h tends to zero the asymptotic limit is clearly achieved. Note also that for "unstable" eigenvalues: $\sigma_j = O(h^2)$ implies that

$$\lambda_j^- = -\sigma_j + O(h^3) \quad \text{and} \quad \lambda_j^+ = 1 + \sigma_j + O(h^3) \tag{24}$$

suggesting that $\lambda^* \to -\sigma_3$ as $h \to 0$.

Grid	$\sigma_3 = \sigma_4$	σ_5	σ_{n^2}
8×8	4.66E-2	7.34E-2	0.9764
16×16	1.32E-2	2.39E-2	0.9941
32×32	3.46E-3	6.63E-3	0.9984
64×64	8.86E-4	1.74E-3	0.9996

Table 1. Behaviour of the eigenvalues σ_j satisfying (5).

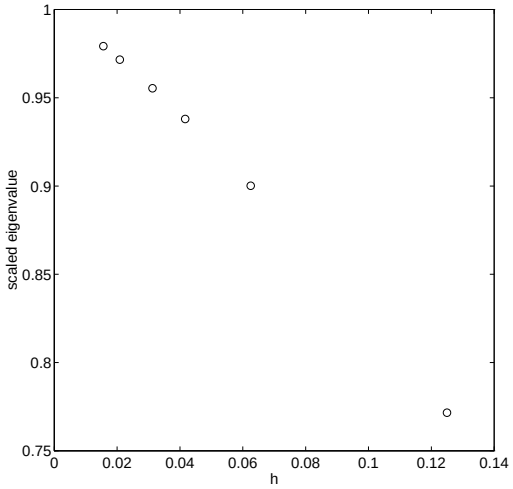

Fig. 1. Behaviour of the scaled maximum negative eigenvalue $-\frac{8}{3}\lambda^*/(\pi^2 h^2)$.

Further confirmation of the analysis in section 2 is given by the contour plots of raw and "demodulated" eigenvectors in figures 2–5. Even with a relatively large value of h, the smoothed pressures in figures 2–4 can be seen to closely approximate the harmonic eigenfunctions: $\bar{p}_{ij} = \cos i\pi x \cos j\pi y$; $i, j = 0, 1$. The "raw" velocity corresponding to the third (nonzero) unstable eigenvalue σ_5 is plotted in figure 6.

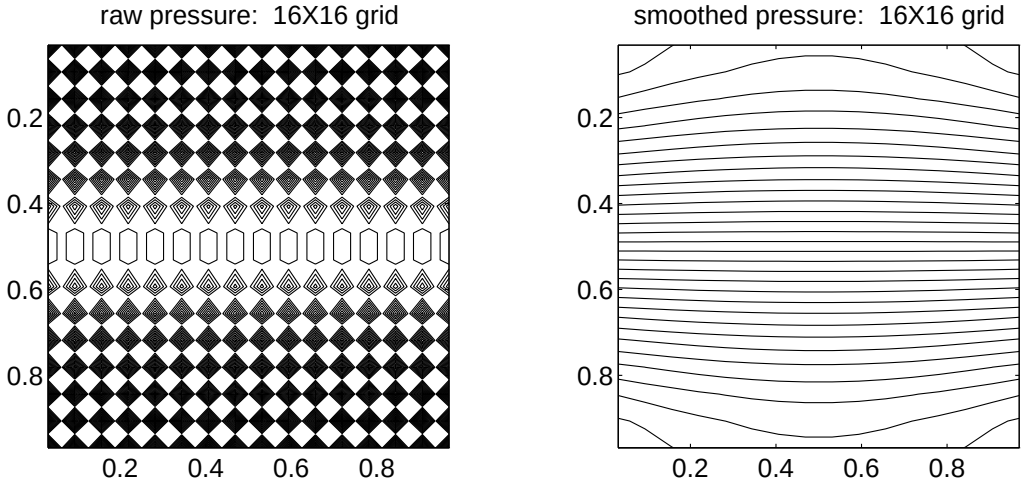

Fig. 2. Contours of pressure component of the first unstable eigenvector corresponding to λ^*.

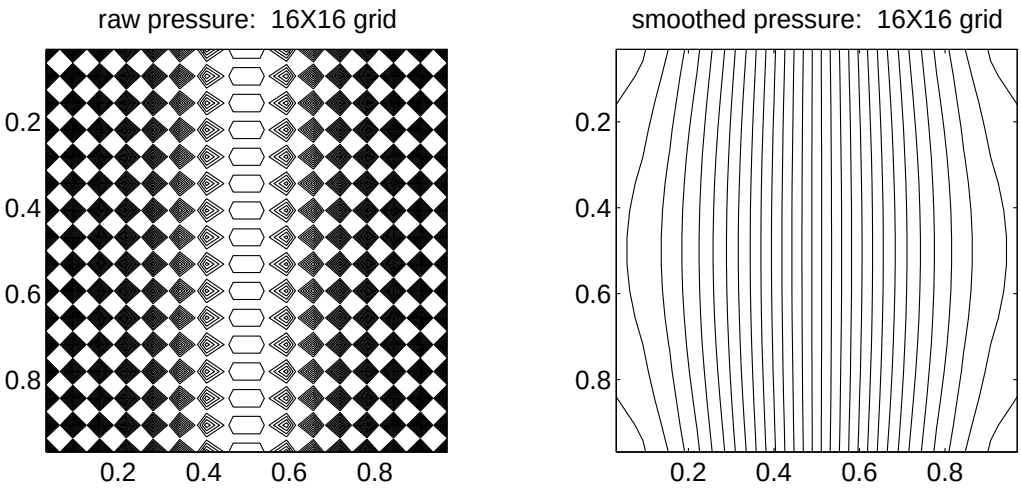

Fig. 3. Contours of pressure component of the second unstable eigenvector corresponding to λ^*.

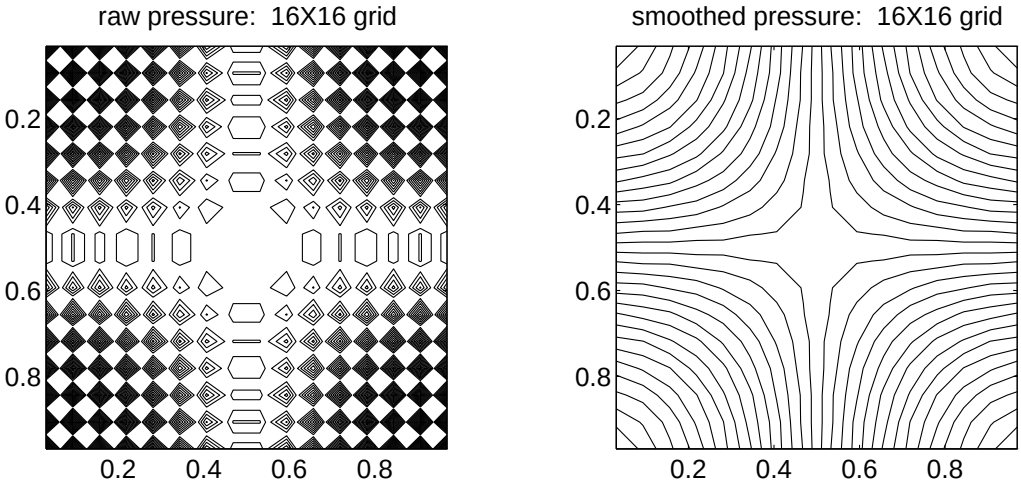

Fig. 4. Contours of pressure component of the unstable eigenvector corresponding to σ_5.

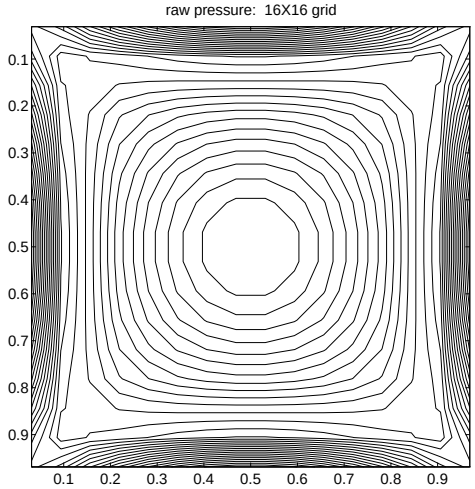

Fig. 5. Contours of pressure component of the eigenvector corresponding to the maximum eigenvalue σ_{n^2}.

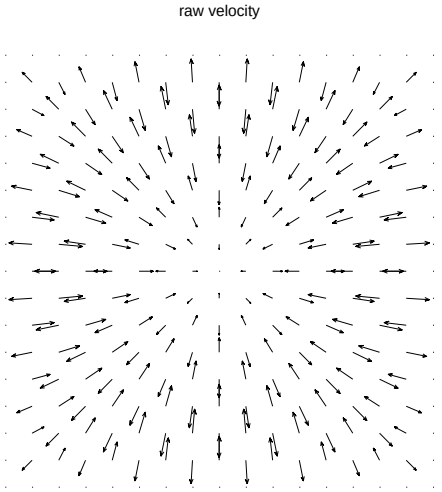

Fig. 6. Velocity component of the unstable eigenvector corresponding to σ_5.

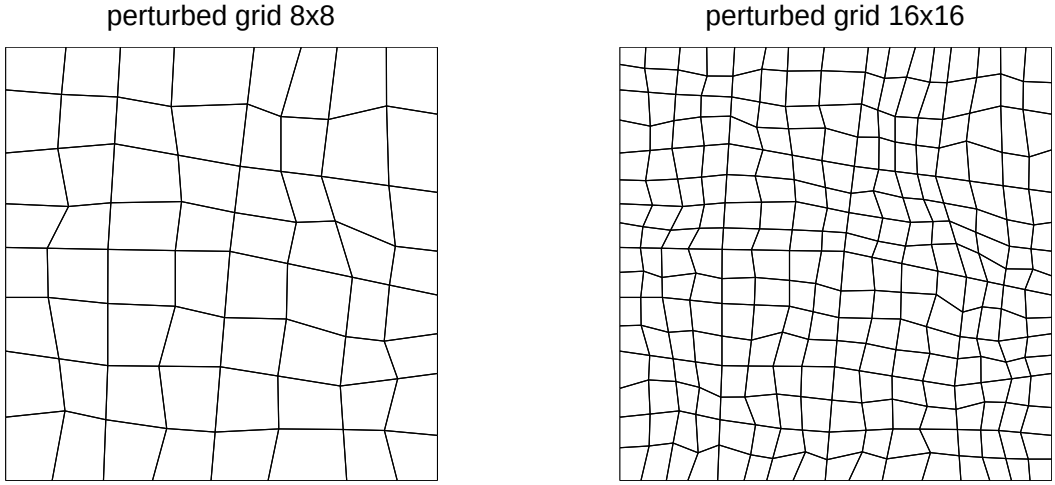

Fig. 7. First two randomly perturbed grids.

It must be emphasised that the "unstable behaviour" in Table 1 is only observed in the case of uniformly refined grids. In fact, cartesian grids of square elements are really the "worst case" possible. It is ironic that the "best" mathematical analysis of Q_1–P_0 [9] is restricted to grids of uniformly refined macroelements. See [5] for further discussion of this issue. It is also worth noting that the instability of Q_1–P_0 can be "removed" by appropriately perturbing an ostensibly uniform grid. To see this, a set of results is given in Table 2, using the nested grid sequence illustrated in figure 7, where at every refinement level the newly introduced nodes (mid-sides and centroid) are randomly perturbed. There is no "spurious" zero eigenmode in this case, furthermore, the non-zero eigenvalues appear to stay bounded away from zero as the mesh is successively refined.

Grid	σ_2	σ_3	σ_4	σ_{n^2}
8×8	5.60E-3	4.49E-2	5.17E-2	0.9755
16×16	1.12E-2	2.04E-2	2.19E-2	0.9935
32×32	1.29E-2	1.44E-2	1.48E-2	0.9984
64×64	1.39E-2	1.49E-2	1.51E-2	0.9996

Table 2. Behaviour of the eigenvalues σ_j
using sequence of randomly perturbed grids.

The instability of section 2 is still apparent, on the other hand, if uniform grids of rectangular

elements are used. In this case the instability is more subtle in that if the aspect ratio is large, λ^* appears to be bounded away from zero on coarse grids. It is only when h is sufficiently small that the $O(h^2)$ asymptotic behaviour of λ^* is observed.

Having established the structure of the underlying instability, the ramifications for practical computations need to be addressed. The critical issue is the effect of the instability on solution accuracy, and the real possibility of discrete solutions blowing up as $h \to 0$, as suggested in [1]. To fix ideas we concentrate on a model test problem: driven cavity flow with zero velocity imposed on three sides of the unit square, with a unit horizontal velocity and zero vertical velocity on the lid. Specifying the horizontal velocity to be unity at the top corners gives a leaky cavity, whereas a value of zero at the corner models the "tough" watertight cavity [10]. In either case, mixed finite element discretisation gives the matrix system

$$\begin{pmatrix} A & 0 & B_x^t \\ 0 & A & B_y^t \\ B_x & B_y & 0 \end{pmatrix} \begin{pmatrix} \mathbf{u} \\ \mathbf{v} \\ \mathbf{p} \end{pmatrix} = \begin{pmatrix} \mathbf{f} \\ \mathbf{0} \\ \mathbf{g} \end{pmatrix}, \tag{25}$$

where $\mathbf{g}$ is identically zero in the leaky cavity case and is non-zero otherwise.

The solution of (25) may be conveniently expressed in terms of the eigenvectors of (7)

$$\begin{pmatrix} \mathbf{u} \\ \mathbf{v} \\ \mathbf{p} \end{pmatrix} = \underbrace{\sum_{j=n_p}^{3} \alpha_j \begin{pmatrix} \mathbf{U}_j \\ \mathbf{V}_j \\ \mathbf{P}_j \end{pmatrix}}_{\lambda<0} + \underbrace{\sum_{k=1}^{n_u-n_p+4} \gamma_k \begin{pmatrix} \mathbf{U}_k \\ \mathbf{V}_k \\ \mathbf{P}_k \end{pmatrix}}_{\lambda=0 \text{ or } \lambda=1} + \underbrace{\sum_{j=3}^{n_p} \beta_j \begin{pmatrix} c_j\mathbf{U}_j \\ c_j\mathbf{V}_j \\ \mathbf{P}_j \end{pmatrix}}_{\lambda>1}. \tag{26}$$

where the eigenvalues defined by (8) are ordered so that

$$\lambda_{n_p}^- \le \ldots \le \lambda_3^- < \lambda_2^- = \lambda_1^- = 0,$$

$$1 = \lambda_1^+ = \lambda_2^+ < \lambda_3^+ \le \ldots \le \lambda_{n_p}^+$$

and all the other eigenvalues are unity. The constants in (26) satisfy

$$c_j = \frac{\lambda_j^- - 1}{\lambda_j^+ - 1} = \frac{\lambda_j^+}{\lambda_j^-},$$

and the amplitude coefficients α_j, β_j are given by

$$\alpha_j \lambda_j^- = \frac{\mathbf{U}_j^t\mathbf{f} + \mathbf{P}_j^t\mathbf{g}}{\mathbf{U}_j^tA\mathbf{U}_j + \mathbf{V}_j^tA\mathbf{V}_j + \mathbf{P}_j^tM\mathbf{P}_j}, \tag{27}$$

$$\beta_j \lambda_j^+ = \frac{c_j\mathbf{U}_j^t\mathbf{f} + \mathbf{P}_j^t\mathbf{g}}{{c_j}^2\mathbf{U}_j^tA\mathbf{U}_j + {c_j}^2\mathbf{V}_j^tA\mathbf{V}_j + \mathbf{P}_j^tM\mathbf{P}_j}, \tag{28}$$

where $M = h^2I$ as in Section 2.

Our goal is then to use the results of Theorem 1 to estimate the projection of the discrete solution onto the locally alternating eigenvectors. For the leaky cavity problem, the right hand side of (27) is zero for the two singular pressure modes (since $\mathbf{U}_j = 0$, $j = 1, 2$ and $\mathbf{g} = \mathbf{0}$), thus the singular system (25) is *consistent*. In addition, the components of $\mathbf{f}$ have the value unity at all interior nodes below the lid (that is for $y = 1 - h$) and are zero otherwise. After rescaling the eigenvector (21) (by multiplying by $\sqrt{2}/\pi$) so that the underlying pressure function $\bar{p}_1$ in (20) has unit L_2–norm, we see that the numerator of (27) corresponding to the leading term in the expansion (26) is given by

$$\mathbf{U}_3^t\mathbf{f} = \begin{cases} (3\sqrt{2}\pi h^2/8)\sin\pi h & \text{if } n \text{ is even,} \\ 0 & \text{if } n \text{ is odd.} \end{cases} \tag{29}$$

From (20) we see that $\mathbf{U}_3^t A \mathbf{U}_3$ is $\mathcal{O}(h^2)$ smaller than $1 = \mathbf{P}_3^t M \mathbf{P}_3 = h\|\mathbf{P}_3\|_2$, so the dominant coefficient in the expansion (26) is of the form

$$\alpha_3 = \frac{1}{\lambda^*}\mathbf{U}_3^t \mathbf{f} + \mathcal{O}(h^2). \tag{30}$$

Combining (30) with (29) and (24) shows that in the worst case (n even, assumed for the remainder of this section)

$$\alpha_3 = \sqrt{2}h + \mathcal{O}(h^2). \tag{31}$$

Similarly it may be shown that the coefficients α_4 and α_5 are both identically zero in this case.

In contrast, the discrete watertight cavity problem is *inconsistent*, since the right hand side of (27) is not zero in the case of the singular chequerboard mode. The crucial difference is that $\mathbf{g}$ has two non–zero components $\pm\frac{1}{2}h$ corresponding to the corner elements adjacent to the driven lid. Furthermore, the unstable pressure vector $\mathbf{P}_3$ has values $\pm\sqrt{2}\cos\frac{1}{2}\pi h$ in the corresponding components, so that $\mathbf{P}_3^t\mathbf{g} = \sqrt{2}h\cos\frac{1}{2}\pi h$. This suggests that the leading coefficient is of the form

$$\alpha_3 = \frac{8\sqrt{2}}{3\pi^2}h^{-1} + \mathcal{O}(1). \tag{32}$$

Numerically computed values of α_3 (ignoring the "lower order" velocity contributions to the denominator in (27)) are presented in Table 3, and can be seen to confirm the coefficient estimates (31) and (32). Our conclusions are thus consistent with prior expectations; in the ill-posed watertight case, the discrete solution blows up like h^{-1} as h is decreased to zero, in contrast, even though the inf-sup constant is still $\mathcal{O}(h)$ the Q_1–P_0 solution *does not* blow up as $h \to 0$ in the leaky case.

	Leaky cavity		Tight cavity	
Grid	α_3	α_3/h	α_3	$\alpha_3 h$
12×12	1.365E-1	1.638	5.906E0	0.4922
16×16	9.791E-2	1.567	7.327E0	0.4579
24×24	6.268E-2	1.504	1.027E1	0.4281
32×32	4.615E-2	1.477	1.327E1	0.4148

Table 3. Numerically computed amplitude coefficients corresponding to the critical eigenvalue λ^*.

Many codes that use the Q_1–P_0 element post–process the pressures using some form of "area–weighted" smoothing [10]. This corresponds in the present context to computing $\mu_x\mu_y P$ at all velocity nodes. Such smoothing would, by the structure of the eigenvectors given in Theorem 1, annihilate the principal component $\alpha_3\mathbf{P}_3$. If pressure smoothing is applied then the first nontrivial contribution in the expansion (26) is for the eigenfunction $\bar{p} = 2\cos 2\pi x \cos \pi y$ of (18), corresponding to $\sigma_8 = 15\pi^2 h^2/8$. Although the coefficient α_8 for the tight cavity is still $\mathcal{O}(h^{-1})$ in this case, the smoothed eigenvector has norm $\mathcal{O}(h^2)$ so the net contribution of the unstable mode is reduced to $\mathcal{O}(h)$.

4. Extensions and Generalisations. In this section we extend the analysis of Section 2 to other related problems. To keep the discussion brief, we focus on the results obtainable, and only describe the technicalities which differ from those in Section 2.

4.1 Q_1–P_0 **Brick elements.** Taking Ω to be the unit cube in three dimensions, the Q_1–P_0 approximation of the eigenvalue problem (12) leads to the system

$$\begin{aligned} -(1-\lambda)\nabla_h^2 U_{\ell,m,n} + h^{-1}\delta_x\mu_y\mu_z P_{\ell,m,n} &= 0,\\ -(1-\lambda)\nabla_h^2 V_{\ell,m,n} + h^{-1}\mu_x\delta_y\mu_z P_{\ell,m,n} &= 0,\\ -(1-\lambda)\nabla_h^2 W_{\ell,m,n} + h^{-1}\mu_x\mu_y\delta_z P_{\ell,m,n} &= 0,\\ -h^{-1}\delta_x\mu_y\mu_z U - h^{-1}\mu_x\delta_y\mu_z V - h^{-1}\mu_x\mu_y\delta_z W &= \lambda P, \end{aligned} \tag{33}$$

where the variables in the final equation are indexed in the obvious way ($U_{\ell+1/2,m+1/2,n+1/2}$, *etc.*), and ∇_h^2 represents the finite difference Laplacian

$$\nabla_h^2 U_{\ell,m,n} = h^{-2}\left[\delta_x^2+\delta_y^2+\delta_z^2+\tfrac{1}{3}\left(\delta_x^2\delta_y^2+\delta_y^2\delta_z^2+\delta_z^2\delta_x^2\right)+\tfrac{1}{12}\delta_x^2\delta_y^2\delta_x^2\right]U_{\ell,m,n}. \tag{34}$$

The analogue of the change of variables (13) is

$$U_{\ell,m,n} = h^3(-1)^{\ell+m+n}\bar{U}_{\ell,m,n}$$

with similar definitions for V and W, and

$$P_{\ell+1/2,m+1/2,n+1/2} = (-1)^{\ell+m+n+1}\bar{P}_{\ell+1/2,m+1/2,n+1/2}.$$

Substituting these into (33) and using the identities

$$\begin{aligned} \mu_x P_{\ell,m,n} &= \tfrac{1}{2}(-1)^{\ell+m+n}\delta_x\bar{P}_{\ell,m,n},\\ \delta_x P_{\ell,m,n} &= 2(-1)^{\ell+m+n}\mu_x\bar{P}_{\ell,m,n},\\ \mu_x U_{\ell+1/2,m+1/2,n+1/2} &= \tfrac{1}{2}(-1)^{\ell+m+n}h^3\delta_x\bar{U}_{\ell+1/2,m+1/2,n+1/2},\\ \delta_x U_{\ell+1/2,m+1/2,n+1/2} &= 2(-1)^{\ell+m+n}h^3\mu_x\bar{U}_{\ell+1/2,m+1/2,n+1/2}, \end{aligned}$$

we find that the resulting equations correspond to a discrete approximation of a modified system which, in the limit $h\to 0$, gives rise to the reduced system

$$\begin{gathered} \tfrac{4}{3}\bar{u}+\tfrac{1}{2}\bar{p}_{yz}=0, \qquad \tfrac{4}{3}\bar{v}+\tfrac{1}{2}\bar{p}_{xz}=0 \qquad \tfrac{4}{3}\bar{w}+\tfrac{1}{2}\bar{p}_{xy}=0,\\ \bar{u}_{yz}+\bar{v}_{xz}+\bar{w}_{xy}=\mu\bar{p}, \end{gathered} \tag{35}$$

in Ω, with $\mu=\lambda/h^4$. The system must also accommodate the boundary conditions $\bar{u}=\bar{v}=\bar{w}=0$ on Γ. The equations (35) imply that each of the variables $\bar{u},\bar{v},\bar{w},\bar{p}$ has to satisfy the eigenvalue problem

$$\phi_{yyzz}+\phi_{zzxx}+\phi_{xxyy}=-\tfrac{4}{3}\mu\phi \qquad \text{in } \Omega \tag{36}$$

for which there is an excess of boundary conditions. Arguing as in Section 2, we need to identify the smallest nonzero eigenvalue, namely

$$\mu=-\tfrac{3}{4}\pi^4+\mathcal{O}(h)$$

which is associated with three eigenfunctions in this case. The first of these has an outer expansion (normalised so that $\|\bar{p}\|_2=1$)

$$\begin{aligned} \bar{u}_1 &= \frac{\mu}{\pi^2}\sin\pi y\sin\pi z\\ \bar{p}_1 &= 2\cos\pi y\cos\pi z \end{aligned} \tag{37}$$

with $\bar{v}_1=\bar{w}_1=0$, and will exhibit boundary layers of width $\mathcal{O}(h)$ along the planes $x=0,1$. The other two eigenfunctions are obtained by simultaneous cyclic permutations of both $(\bar{u},\bar{v},\bar{w})$ and (x,y,z). We summarise in the form of a theorem.

THEOREM 3. *The inf-sup constant for Q_1–P_0 approximation of (1) in three dimensions is given by*

$$\sqrt{\sigma} = \tfrac{1}{2}\sqrt{3}\pi^2 h^2 + \mathcal{O}(h^3).$$

The corresponding eigenspace has dimension three and is spanned by mutually orthogonal eigenvectors which may be deduced from (37).

It would appear from the above that the Q_1–P_0 brick element is more unstable than it's two dimensional analogue, by an order of h. This is not necessarily so however, solving the consistent leaky three dimensional driven cavity ($u = 1, v = w = 0$ on the plane $z = 1$), the coefficient of the critical eigenmode analogous to (30) is of the form

$$\alpha^* = 2h + \mathcal{O}(h^2)$$

which is the same order of h as (31). On the other hand, for the tight cavity, where $u = v = w = 0$ along the leading and trailing edges of the lid, we find that

$$\alpha^* = \frac{8}{3\pi^4} h^{-2} + \mathcal{O}(h^{-1})$$

in which case the instability is indeed more severe than in two dimensions.

4.2 Inf–Sup Stability of L_2 Projection Methods. A number of (semi-)explicit integration methods for the time–dependent Navier-Stokes equations force incompressibility by projecting the discrete velocity field onto the associated divergence-free subspace. Working with the standard L_2 projection, the associated pressure may be computed from a "pressure Poisson equation", of the form (5) except that the matrix K is either the mass matrix of the velocity space [3] (section 9), or else is a "lumped" approximation thereof [4].

To study the inf-sup stability of the L_2 projection in the Q_1–P_0 case, we express the associated eigenproblem (cf. (10)) in finite difference form

$$\begin{aligned}
(1-\lambda)(1+\tfrac{1}{6}\delta_x^2)(1+\tfrac{1}{6}\delta_y^2)U_{\ell,m} + h^{-1}\delta_x\mu_y P_{\ell,m} &= 0,\\
(1-\lambda)(1+\tfrac{1}{6}\delta_x^2)(1+\tfrac{1}{6}\delta_y^2)V_{\ell,m} + h^{-1}\mu_x\delta_y P_{\ell,m} &= 0,\\
-h^{-1}\delta_x\mu_y U_{\ell+1/2,m+1/2} - h^{-1}\mu_x\delta_y V_{\ell+1/2,m+1/2} &= \lambda P_{\ell+1/2,m+1/2},
\end{aligned} \tag{38}$$

and view it as a consistent approximation of

$$\begin{aligned}
\mathbf{u} + \nabla p &= \lambda \mathbf{u},\\
-\nabla\cdot\mathbf{u} &= \lambda p,
\end{aligned} \tag{39}$$

in Ω, with $\mathbf{u} = \mathbf{0}$ on Γ. Like (12), the system (39) has one eigenvalue $\lambda = 0$ corresponding to the hydrostatic mode $\mathbf{u} = \mathbf{0}, p =$ constant, and an eigenvalue $\lambda = 1$ of infinite multiplicity with corresponding eigenfunctions satisfying $\nabla\cdot\mathbf{u} = 0$, $p = 0$. It is different from (12), however, in that it has no nontrivial irrotational eigenvectors. The system (38) may also be viewed as a consistent approximation to order $\mathcal{O}(h^2)$ of the singularly perturbed system

$$\begin{aligned}
(1-\lambda)\left[\mathbf{u} + \tfrac{1}{6}h^2\nabla^2\mathbf{u}\right] + \nabla p &= \mathbf{0} \qquad \text{in } \Omega,\\
-\nabla\cdot\mathbf{u} &= \lambda p \qquad \text{in } \Omega,\\
\mathbf{u} &= \mathbf{0} \qquad \text{on } \Gamma
\end{aligned} \tag{40}$$

where only second derivative terms are retained, since the retention of higher derivatives would require additional boundary conditions. The system (39) clearly provides a reduced system for (40), furthermore, the boundary conditions may be relaxed by the introduction of suitable boundary layers, to involve only

the normal component of velocity. In this case the pressure eigenfunctions of the reduced system are those of the Neumann problem, and the eigenvalues then satisfy $\lambda(\lambda-1)=\sigma$, where

$$\sigma = (j^2+k^2)\pi^2, \qquad j,k = 0,1,2,\ldots \tag{41}$$

has multiplicity two for $j \neq k$. Clearly one of the eigenfunctions is given by

$$\begin{pmatrix} u \\ v \\ p \end{pmatrix} = \begin{pmatrix} j\pi \sin j\pi x \cos k\pi y \\ k\pi \cos j\pi x \sin k\pi y \\ (1-\lambda)\cos j\pi x \cos k\pi y \end{pmatrix} \tag{42}$$

and the other is obtained by interchanging j and k.

A second set of eigenvalues may be deduced by substituting

$$\begin{aligned} U_{\ell,m} = (-1)^{\ell+m}\bar{U}_{\ell,m}, \qquad V_{\ell,m} = (-1)^{\ell+m}\bar{V}_{\ell,m}, \\ P_{\ell+1/2,m+1/2} = (-1)^{\ell+m+1}\bar{P}_{\ell+1/2,m+1/2}, \end{aligned} \tag{43}$$

into (38). These substitutions differ from (13) in that the velocities are no longer scaled by h^2. Following the procedure described in Section 2 we obtain the reduced equations

$$\begin{aligned} \tfrac{1}{9}(1-\lambda)\bar{\mathbf{u}} + \nabla\bar{p} &= \mathbf{0}, \\ -\nabla\cdot\bar{\mathbf{u}} &= \lambda\bar{p}, \end{aligned}$$

whose eigenvalues now satisfy $\lambda(\lambda-1)=9\sigma$, with σ given by (41), and the corresponding eigenfunctions $(\bar{u},\bar{v},\bar{p})$ again are of the form (42). This gives our final theorem.

THEOREM 4. *Using Q_1–P_0 approximation on a square $n\times n$ grid, the discrete L_2 projection problem*

$$BK^{-1}B^t\mathbf{P} = \sigma M\mathbf{P}, \tag{44}$$

with K the velocity mass matrix, has eigenvalues given by

$$\sigma \approx (j^2+k^2)\pi^2, \quad \textit{and} \quad \sigma \approx 9(j^2+k^2)\pi^2, \qquad j,k = 0,1,2,\ldots \tag{45}$$

(for values of j and k that are small compared with n), and corresponding eigenvectors with pressure components

$$P_{\ell,m} \approx \cos\pi j\ell h \cos\pi kmh \quad \textit{and} \qquad P_{\ell,m} \approx (-1)^{\ell+m+1}\cos\pi j\ell h\cos\pi kmh,$$

and velocity components which may be deduced from (42) and (43).

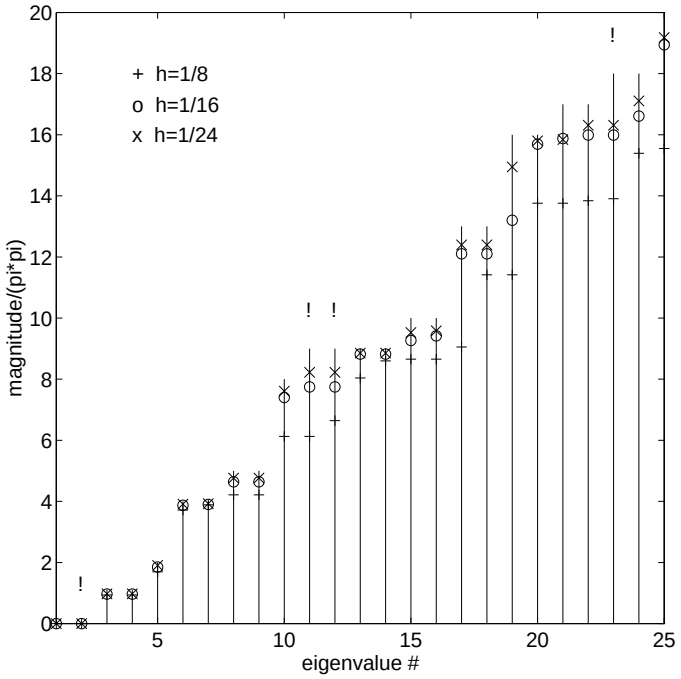

Fig. 8. Comparison of analytic vs. computed eigenvalues of the L_2 pressure projection equation.

Some numerical results which confirm our analytic estimates are presented in figure 8, where we plot the first 25 scaled eigenvalues σ/π^2 for a range of values of h. The vertical lines depict the predicted eigenvalues from Theorem 4, and the symbol ! above particular eigenvalues indicate those in the set (45) which have locally alternating eigenvectors.

When the velocity mass matrix is "lumped", the operator $(1+\frac{1}{6}\delta_x^2)(1+\frac{1}{6}\delta_y^2)$ in (38) may be replaced by the identity. The velocities can then be eliminated from the resulting system giving a discrete eigenvalue problem for the pressure, which is the usual 5–point finite difference replacement of the Laplacian rotated through 45°. It follows that the pressures on "red" and "black" elements are unconnected. However, the equation for the pressure cannot be treated in isolation since the boundary conditions are imposed through the velocites. When these effects are taken into account, the only change in the statement of Theorem 4 is that the factor 9 in (45) is absent. Thus, in contrast to the "consistent mass" projection, oscillatory and smooth eigenvectors are present in pairs in the lumped mass case. That is each eigenvalue has multiplicity two for $j = k$ and multiplicity four otherwise, with associated eigenvectors as given in Theorem 4.

5. Conclusions. In this work we have analysed two fundamental properties of Q_1–P_0 approximation on uniform grids. Firstly, in two and three dimensions, the inf–sup constant for the Stokes (H^1–) projection tends to zero with h, when it needs to be bounded away from zero in order to be stable in the standard sense. The projection of the unstable eigenmodes onto the boundary data is sufficiently small however, that convergence to the true solution as $h \to 0$ is still possible in cases of physical interest. Secondly, the inf-sup constant associated with the L_2–projection is bounded away from zero, although the eigenspace of the projection operator is still contaminated by unstable eigenmodes which are identical to those arising in the Stokes projection.

REFERENCES

[1] J. Boland and R. Nicolaides. On the stability of bilinear–constant velocity–pressure finite elements. *Numer. Math.*, 44:219–222, 1984.

[2] F. Brezzi and M. Fortin. *Mixed and Hybrid Finite Element Methods*. Springer-Verlag, New York, 1991.

[3] M. Fortin. Finite element solution of the Navier-Stokes equations. In A. Iserles, editor, *Acta Numerica 1993*. Cambridge University Press, 1993.

[4] P. Gresho. On the theory of semi-implicit projection methods for viscous incompressible flow and its implementation via a finite element method that introduces a nearly consistent mass matrix. *Internat. J. Numer. Methods Fluids.*, 11:587–620, 1990.

[5] P. Gresho, R. Sani, and M. Engelman. *Incompressible Flow and the Finite Element Method*. Wiley, New York. to appear.

[6] C. Johnson and J. Pikäranta. Analysis of some mixed finite element methods related to reduced integration. *Math. Comp.*, 38:375–400, 1982.

[7] J. Kevorkian and J. Cole. *Perturbation Methods in Applied Mathematics*. Springer-Verlag, New York, 1981.

[8] D. Malkus. Eigenproblems associated with the discrete LBB condition for incompressible finite elements. *Int. J. Eng. Sci.*, 19:1299–1310, 1981.

[9] J. Pitkäranta and R. Stenberg. Error bounds for the approximation of the Stokes problem using bilinear/constant elements on irregular quadrilateral meshes. In J. Whiteman, editor, *The Mathematics of Finite Elements and Applications V*, pages 325–334, London, 1985. Academic Press.

[10] R. Sani, P. Gresho, R. Lee, and D. Griffiths. The cause and cure(?) of the spurious pressures generated by certain finite element method solutions of the incompressible Navier-Stokes equations. *Internat. J. Numer. Methods Fluids.*, 1:17–43, 1981.

[11] D. Silvester. Optimal low order finite element methods for incompressible flow. *Comput. Methods. Appl. Mech. Engrg.*, 111:357–368, 1994.